Chapter 14
Challenges in Dimensioning of an Optimized Thermoelectric Generator for Waste Heat Recovery in Cars

M. Rauscher, T. Richter, F. Finsterwalder, and D. Schramm

Abstract An exhaust system in a car has to face and withstand a lot of different operating conditions and so does a thermoelectric generator (TEG) integrated in the exhaust system. In addition, the TEG has to transform heat into electricity at the highest possible efficiency in order to save fuel. This results in several challenges with regard to the design and the dimensioning of the TEG.

One lever to improve the efficiency of a TEG is the optimization of the thermal resistance of the thermoelectric material. This paper shows performance data of TE modules made of identical material and active area but of different thickness. These modules have been measured under thermostatic conditions, i.e., fixed surface temperatures. Subsequently the different TE modules have been tested in a hot air test bench. Here, the consequences of the different thermal resistances can be shown. Furthermore the measurements highlight the influence of the electric load on the thermal resistance of the module entailing different surface temperatures of the modules and different heat transfer rates.

Along with the experimental tests, numeric optimization of the thermal resistances of the TE modules has been carried out in order to achieve the maximum electrical power output. The optimum module thermal resistance significantly depends on whether the power output of the modules is optimized individually or if the power generation of TEG is optimized as a whole.

Keywords Thermoelectric generator • Waste heat recovery • Thermal resistance • Optimization

M. Rauscher (✉) • T. Richter • F. Finsterwalder
Daimler AG, Ulm, Germany
e-mail: matthias.rauscher@daimler.com

D. Schramm
Universität Duisburg-Essen, 47057 Duisburg, Germany

A. Amaldi and F. Tang (eds.), *Proceedings of the 11th European Conference on Thermoelectrics: ECT 2013*, DOI 10.1007/978-3-319-07332-3_14,

List of Symbols

A	Module surface
A_{tem}	Surface of thermoelectric material in a module
P_x	Electric power output in segment x (W)
$\dot{Q}_x$	Heat flow rate into the thermoelectric material in segment x (W)
R_x^{hs}	Thermal resistance from the exhaust gas to the thermoelectric material in segment x (K m²W^{-1})
R_x^{tem}	Thermal resistance of the thermoelectric module in segment x (K m²W^{-1})
R_x^{cs}	Thermal resistance from the thermoelectric material to the coolant in segment x (K m²W^{-1})
T_x^{g}	Temperature of the exhaust gas in segment x (K)
T_x^{c}	Temperature of the coolant in segment x (K)
$T_x^{tem,hs}$	Temperature at the hot side of the thermoelectric material in segment x (T)
$T_x^{tem,cs}$	Temperature at the cold side of the thermoelectric material in segment x (T)
$T_{CS,HS}$	Positions of temperature measurements at the cold side and the hot side of the thermoelectric module
$T_{HS1,2,3}$	Positions of temperature measurements in the cube of the hot side
$T_{CS1,2,3}$	Positions of temperature measurements in the cube of the cold side
η_x	Efficiency of the thermoelectric material in segment x

Introduction

The limitation of crude oil, the rising petrol price during the last years, as well as legislation requires a drastic reduction of vehicle fuel consumption. State-of-the-art vehicles with modern combustion engines still produce more waste heat than they convert into mechanical energy [1]. An important field of research is therefore the recovery of waste heat, for example using thermoelectric materials. In this regard, the exhaust gas is particularly attractive due to its generally high energy content at elevated temperatures, although this varies strongly over a drive cycle turning the dimensioning and the design of the TEG in a demanding exercise. Small packaging and minimized weight and costs are further targets of the automotive industry. Within these boundaries the TEG must work at the highest possible performance.

As a consequence the module design has to be adapted to the heat exchanger, e.g., by changing the height or the surface area of the thermoelements (legs) of the modules. An increase of the leg height leads to a higher thermal resistance of the module and therefore to a reduced heat flux and a higher efficiency within a TEG. The same effect is obtained when the surface area is reduced in the direction of the heat flux in a leg. For this purpose a small demonstrator TEG has been built. This TEG is not intended to be used in a car, but allows getting insight into the behavior of different module designs.

Test Bench Results

Two thermoelectric modules of the same contact area, identical thermoelectric material (bismuth telluride) but different height of the legs (see Table 14.1), have been tested under thermostatic conditions in a module test bench at different hot and cold side temperatures.

The different module designs result in a different thermoelectric behavior of the modules. The higher number of legs in module A leads to a higher open voltage compared to module B at the same surface temperature. Simultaneously, the electrical resistance of module A is higher owing to the number of legs, which are electrically in series, and the higher geometric factor (ratio of leg length to leg footprint). Due to the same ratio of thermoelectrically active surface compared to the module surface, but the higher geometric factor, module A has a smaller thermal resistance, which results in a higher heat flux through the module compared to module B. Figure 14.1 shows the test setup of both modules at the module test bench.

Table 14.1 Module basic data

	Module surface (cm^2)	Ratio: A_{tem}/A	Geometric factor of the legs (mm^{-1})
Module A	16	ca. 0.5	0.83
Module B	16	ca. 0.5	0.75

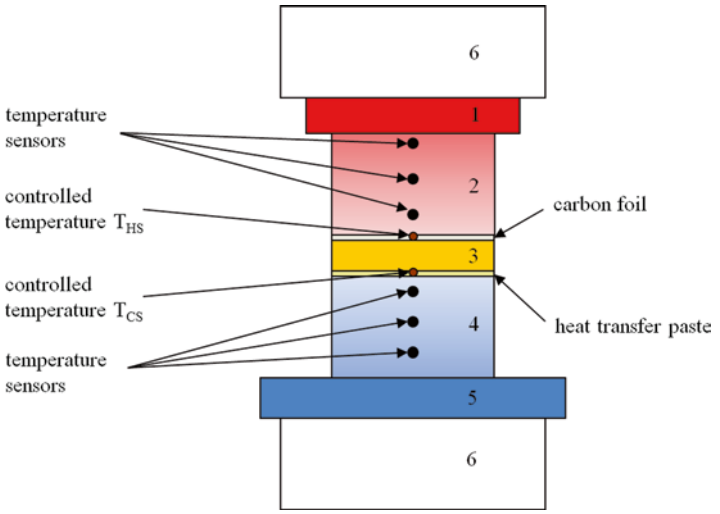

Fig. 14.1 Test bench Setup: Module test bench (1) Cooling plate, (2) aluminum cube, (3) thermoelectric module, (4) copper cube, (5) heating plate, (6) isolating stone

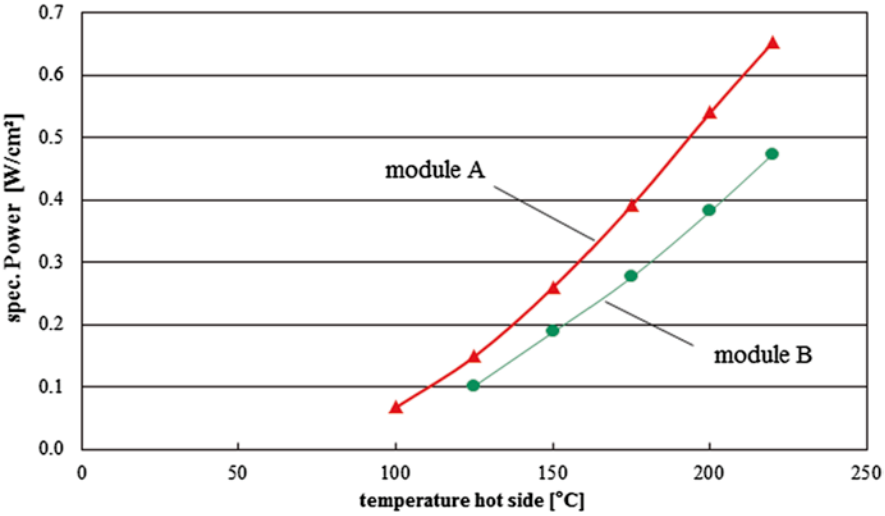

Fig. 14.2 Electrical power output of module A and B at fixed surface temperatures (the cold side temperature was 50 °C)

The applied contact pressure was 10 bars. The electrical contacts have been connected to an electrical load. To measure the maximal power output, the current of the electric load was successively increased until the electrical power output reached its maximum. The temperatures on the hot and cold side of the module have been readjusted during the measuring procedure. Figure 14.2 illustrates the power output in the maximum power point of the two modules for a cold side temperature of 50 °C and various hot side temperatures in the range of 100–220 °C.

Over the range of hot side temperatures the maximum electric power output of module A is around 1.33 times higher than the maximum electrical power output of module B. This is due to the decreased thermal resistance of module A as a consequence of the reduced leg height.

Figure 14.3 shows the heat flux into the modules in the maximum power point. The heat flux has been calculated using the measured temperature differences, the surface of the cube, and the known thermal conductivity of the copper cube shown in Fig. 14.1. At the same operating temperatures the heat flux into module A is also ca. 1.33 higher than the heat flow rate into module B. Again, this is a result of the reduced thermal resistance of module A.

Obviously, the efficiency is nearly the same, as one would expect from modules made of identical materials and layer composition.

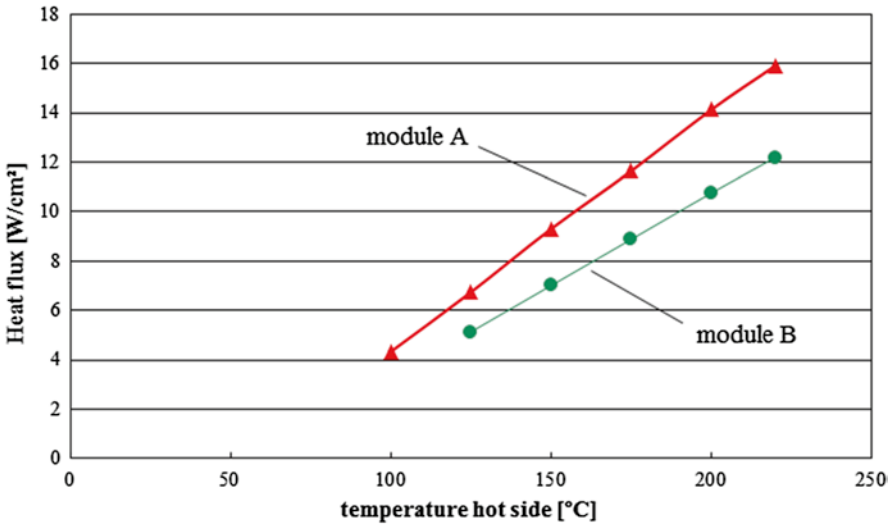

Fig. 14.3 Test results for heat flux of module A and B for fixed surface temperatures (the cold side temperature was 50 °C)

Hot Air Test Bench Results

The previously described thermoelectric modules (type A and B) have been integrated in a heat exchanger of which the setup is shown in Fig. 14.4.

The TEG has one gas channel and two channels for the coolant. The TE modules are inserted between the gas and the liquid side: three modules of type A on the upper half of the heat exchanger and three modules of type B on the lower half. Two thermocouples (inserted in pockets punched into the graphite foils) have been positioned on each module, one on the hot and one on the cold side.

The TEG has been tested under steady-state conditions. The gas (dry air) inlet temperature was 320 °C and the coolant (water glycol mixture) temperature was 40 °C.

Table 14.2 shows the surface temperatures module A1 and B1 at open electrical circuit. Due to the higher thermal resistance of module B1, the temperature difference between hot and cold side is larger for B1 than for A1.

The electric power output of the modules has been determined using a variable electronic load. As in the test setup in the module test bench, the electronic load increases the electrical current from zero to maximum within 4 min. The maximum power point has been tracked for all modules individually.

Figure 14.5 illustrates the surface temperature and the electric current while changing the electric current from zero to its maximum. In this case, the load has only been applied to module B1. The temperature on the hot side of B1 decreases with increasing current, while the corresponding temperature on the cold side increases. The reason is that the heat transport of the module B1 has changed because of the Peltier, Joule, and

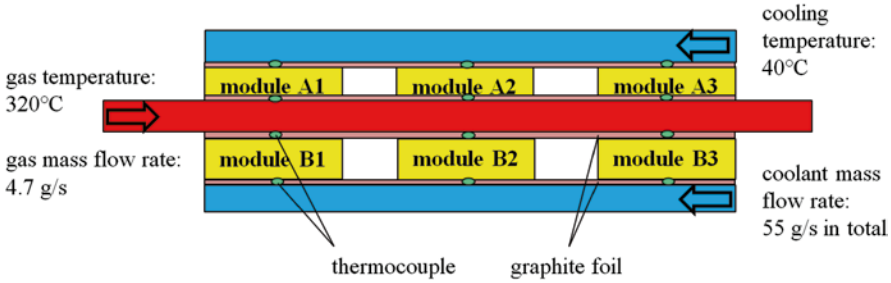

Fig. 14.4 Schematic of the TEG demonstrator unit (side view)

Table 14.2 Module surface temperatures

	Measured surface temperature hot side (°C)	Measured surface temperature cold side (°C)	Temperature difference (K)
Module A1	197	118	79
Module B1	211	111	100
Module A2	168	101	67
Module B2	178	100	78

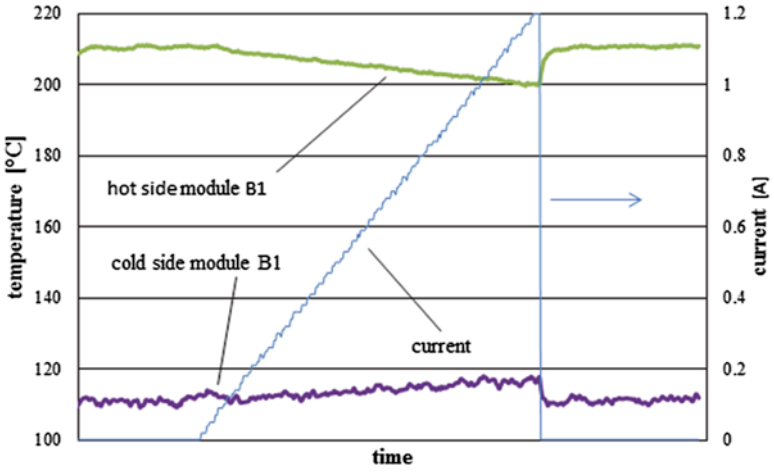

Fig. 14.5 Dependence of the surface temperature of module B1 on the electric load

Thomsen effect. When the electric load is removed, the surface temperatures of the module return to their initial values.

The maximum power outputs of modules B exceed the corresponding maximum power of the neighboring modules A by the factor of 1.22–1.53, depending on their position in the TEG. This is in contrast to the power outputs measured under fixed

surface temperatures (see Fig. 14.2), where the type B modules have shown inferior performance. Here, the type B modules (integrated in the heat exchanger) have a higher temperature gradient between the hot and the cold side as a result of the higher thermal resistance of the module. This leads to an increased efficiency (electrical output power divided by ingoing heat flux) of the module. In this case, the higher efficiency of the module overcompensates the reduced heat flow across the module (due to the higher thermal resistance) resulting in an overall superior maximum electrical power output.

Numerical Optimization of the Thermal Module Resistance for Maximum Power Output

As can be seen from the previous results the thermal resistance is a key parameter with regard to the electrical power output. Its optimization plays a vital role in the design process of an automotive TEG. The following section describes a numerical approach for the optimization of the thermal resistance to get the highest yield of electrical power.

The optimum thermal resistance, determined by the aspect ratio of the legs of the module, can be determined relatively easily for a single module with no lateral temperature gradient using thermoelectric equations [2, 3]. However, the calculation becomes much more complicated when lateral temperature gradients occur within the TEG (usually consisting of several module segments, see Fig. 14.6) along the flow direction of the hot and cold media [4]. As a result, the efficiency as well as the local power generation varies.

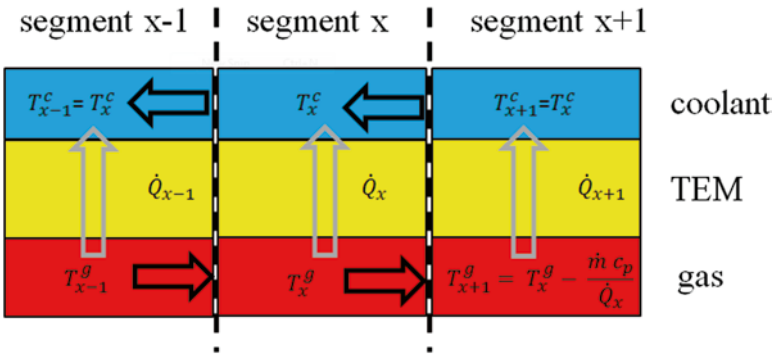

Fig. 14.6 Schematic model of the TEG

For this case, we assume that the identical material (PbTe) is used in every segment of the TEG and we suppose a constant heat transfer coefficient (R_x^{hs}, R_x^{cs}) for both gas and coolant side. The module segments are considered discretely, so we assume there is no electrical interaction between the segments.

The heat flow rate of each of the segments (see Fig. 14.6) of the TEG has been calculated by using Eq. (14.1).

$$\dot{Q}_x = A \frac{1}{R_x^{hs} + R_x^{tem} + R_x^{cs}} \left(T_x^g - T_x^c \right) \tag{14.1}$$

$$T_{x+1}^g = T_x^g - \frac{\dot{m}_g \cdot c_p}{\dot{Q}_x} \tag{14.2}$$

The temperature of the coolant is set to a constant value. This simplification is done because of the much higher mass flow and heat capacity compared to the gas, so that the warming of the coolant can be neglected.

The temperatures $T_x^{tem,cs}$ and $T_x^{tem,hs}$ can be calculated from the ratio of the thermal resistances in each segment. For the calculation of the electric power output the following equations [5] were used.

$$\eta_x = \frac{\sqrt{1 + ZT_x} - 1}{\sqrt{1 + ZT_x} + \frac{T_x^{tem,cs}}{T_x^{tem,hs}}} \cdot \frac{T_x^{tem,hs} - T_x^{tem,cs}}{T_x^{tem,hs}} \tag{14.3}$$

$$P_x = \eta_x \cdot \dot{Q}_x \tag{14.4}$$

Equation (14.3) assumes that the electric current in a segment is adapted in the way that the thermoelectric material works at maximum efficiency.

For the calculation of the temperature-dependent ZT_x value the average temperature of the thermoelectric material in the segment has been used. This simplification can still be employed with an acceptable degree of accuracy [5].

Three different optimization methods of the thermal resistance R^{tem} of the modules have been employed:

1. Maximization of the electric power output of *every single* segment:
   The thermal resistance R^{tem} of each individual segment is adapted in the way that the maximum electrical power of the segment is generated using the locally available waste heat energy. The calculation is started with the segment nearest to the gas inlet.
2. Maximization of the electric power output of the *complete TEG*:
   The thermal resistance R^{tem} of each individual segment is adapted in a way that the added electrical power output of all segments becomes a maximum.
3. Maximization of the electric power output of the *complete TEG*:
   The thermal resistances R^{tem} of all segments are equal and adapted in a way that the added electrical power output of all segments becomes a maximum.

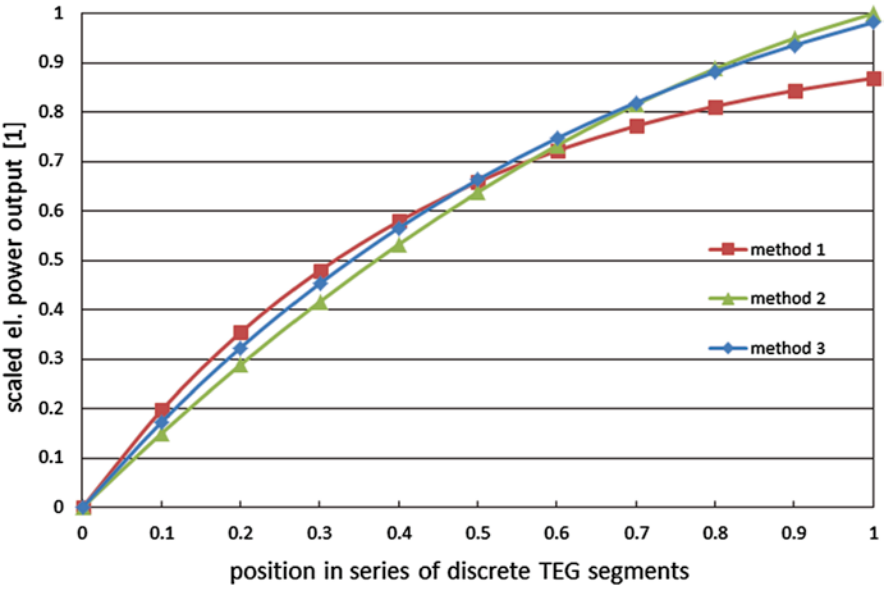

Fig. 14.7 Cumulated electrical power output as a function of the scaled length of the TEG

For all three methods, the optimal thermal resistances were calculated using an iterative algorithm (Generalized Reduced Gradient [6]). The results of the different methods of electrical power optimization along the TEG are shown in Fig. 14.7. The *y*-axis is normalized to the electrical power output of method 2.

Within the first half of the TEG, the optimization method 1 gives the highest electric power output. The reason is that the TEG optimized by method 1 cools down the exhaust gas relatively strongly at the inlet (maximum electrical power generation of each segment), so that the remaining amount of heat for the downstream segments is relatively low. Therefore the first segments produce much electrical power at relatively low efficiency at the expense of the following segments. The decline in power generation of each segment is more pronounced than in the other cases where the power drop is less steep.

The thermoelectric segments of the TEG optimized by method 2 have got a much higher thermal resistance in the inlet area. Therefore the heat flow is reduced and the electric power output is lower despite the higher efficiency. Hence, the available gas temperature and energy for the downstream segments is higher. This entails a superior power output in the remaining segments in comparison to method 1. Apparently, the overall power output of the TEG optimized according to method 2 is higher than that when using method 1 (in this operating point the gain in power amounts to approximately 13 %).

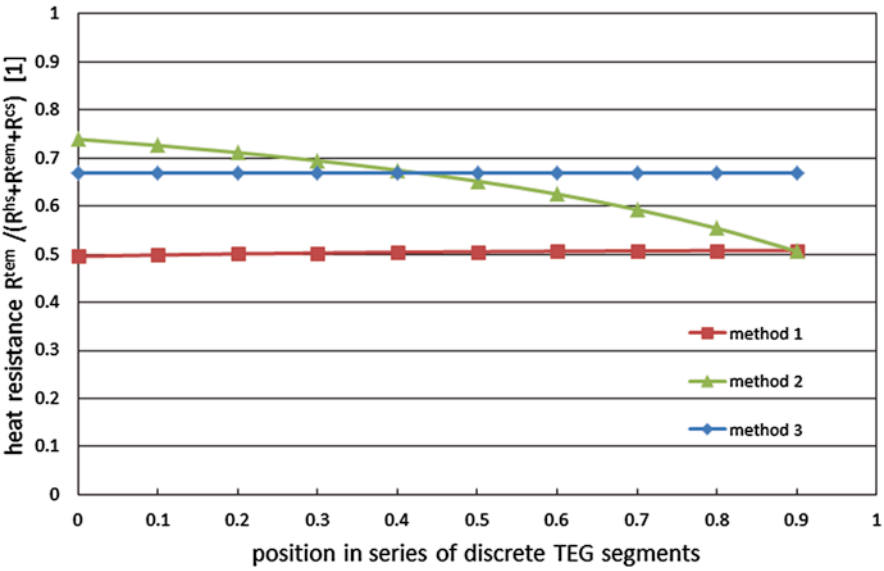

Fig. 14.8 Segment heat resistance along the TEG for different optimization methods

Optimization method 3 implies identical module resistances along the TEG (see Fig. 14.8). The optimized resistance throughout the TEG is clearly higher than the resistances resulting from method 1, which show only very little variation. Compared to method 2, the resistance at the beginning of the TEG is lower, whereas the resistance at the outlet of the TEG is higher.

In total, electric power output for method 3 is only 2 % lower than for method 2 despite the additional boundary condition of constant resistance.

Note that the calculations refer only to one operating point, which is however typical for the curve progression. Changes of the operating parameters lead to changes in the absolute values of the optimized thermal resistances but the general trend, i.e., the strongly digressive power output along the TEG when using method 1, remains. In all chosen boundary conditions for the exhaust gas mass flow or temperature, method 1 leads to the lowest average thermal resistance compared to the other methods. Method 2 has always the highest thermal resistance at the beginning of the TEG and decreases towards the end.

The differences in the results of the optimization methods shrink with a smaller gas temperature gradient from the entry to the exit of the TEG. This may be caused by higher mass flows or a shorter TEG. Vice versa, the differences in the results increase at lower mass flows or a longer TEG design. In the limiting case, i.e., no gas temperature gradient along the TEG, all three methods yield the same result; hence in this case all segments in the TEG have equal boundary conditions and therefore the optimization methods have the same optimization goal.

Summary

The measurements of two different modules made of the same material but different aspect ratio of the legs integrated in a demonstrator TEG have highlighted the crucial impact of the thermal resistance on the electrical power generation. An adaption and optimization of the module heat resistances to the heat exchanger is therefore essential.

Simulations show that individual optimization of module heat resistances is not necessary, but the optimum TEG power output performance can almost be achieved, if all modules have the same heat resistance, i.e., the same design. This result is equally important and encouraging. A cost-effective mass production of TEGs is easier if a single module design is used.

Under the considered boundary conditions the simulation has also revealed that a power optimization of every single module is less beneficial and comes at the expense of the overall TEG power output. Instead, the module heat resistance should be optimized with respect to the total TEG power output.

References

1. Steinberg P, Briesemann S, Goßlau D (2009) Thermoelectrics goes automotive, Der Fahrzeugmotor als Energielieferant fürWärmenutzungskonzepte. IAV, Renningen
2. Glatz W, Muntwyler S, Hierold C (2006) Optimization and fabrication of thick flexible polymer based micro thermoelectric generator. Sens Actuators A 132:337–345
3. Beckert W, Dannowski M, Wagner L. Symposium Thermoelektrik Dresden. Simulations werkzeuge zur Unterstützung der Integration thermo-elektrischer Generatoren in bestehende Systeme
4. Roy G, Matagne E, Jacques PJ (2013) A global design approach for large-scale thermoelectric energy harvesting systems. J Electron Mater 42(7):1781–1788
5. Rowe DM (2006) Thermoelectrics handbook “general principles and basic considerations”. Taylor & Francis Group, New York, pp 11–114
6. Lasdon LS, Waren AD, Jain A, Ratner M (1978) Design and testing of a generalized reduced gradient code for nonlinear programming. ACM Trans Math Softw 4:34–50